

## Heat Transfer Management of Thermal and Electronics Systems using Convective-Radiative Porous Fins with Thermal Contact Resistance and Diabatic Tip

Article Info:

Article history: Received 2024-02-22 / Accepted 2024-07-01 / Available online 2024-07-01

doi: 10.18540/jcecv110iss5pp18523



**Joy Nneka Ojuro**

ORCID: <https://orcid.org/0009-0005-0775-6200>

Department of Computer Science, University of Louisiana,  
Lafayette, USA

E-mail: [ojurojoy@gmail.com](mailto:ojurojoy@gmail.com)

**Gbeminiyi Musibau Sobamowo**

ORCID: <https://orcid.org/0000-0003-2402-1423>

Department of Mechanical Engineering, Faculty of Engineering, University of Lagos, Akoka  
Department of Mathematics, Faculty of Science, University of Lagos, Akoka  
Lagos, Nigeria

E-mail: [gsobamowo@unilag.edu.ng](mailto:gsobamowo@unilag.edu.ng)

**Antonio Marcos de Oliveira Siqueira**

ORCID: <https://orcid.org/0000-0001-9334-0394>

Federal University of Viçosa, Brazil

E-mail: [antonio.siqueira@ufv.br](mailto:antonio.siqueira@ufv.br)

### Abstract

The miniaturization of electronics, electrical, thermal, mechanical and optical devices and systems calls for increasing demand for efficient cooling systems with higher thermal efficiency. The use of passive mode of cooling using fins has provided unprecedented results. However, the previous transient analyses of the extended surfaces have been done without proper considerations of the imperfect contact between the fin base and the prime surface. Also, the tip of the passive device has been assumed to be adiabatic. However, the present article explores the significances of thermal contact resistance and diabatic tip on the transient thermal response of straight fin with temperature-dependent thermal conductivity and magnetic field under radiative-convective conditions. The nonlinear model is analysed numerically using generalized Integral Transform Techniques and the numerical results are verified by the exact solution for the linear thermal model. The parametric explorations reveal that the dimensionless local temperature in the conductive-radiative fin increases when the conductive-convective, conductive-radiative and magnetic field parameters increase. However, under the assumption of perfect thermal contact between the prime surface and the base of the fin, the dimensionless temperature in the fin will decrease as the conductive-convective, conductive-radiative and magnetic field parameters increase. The fin temperature is significantly affected by the Biot numbers under the comparably low values of the conductive-convective, conductive-radiative, magnetic field and thermal conductivity parameters. The effects of the fin thermal conductivity parameter along the fin length depend on the respective values of thermal contact Biot number at the base of the fin and the end cooling Biot number at the tip of the fin. When the thermal conductivity parameter is amplified, the fin dimensionless temperature increases when thermal contact Biot number at the base of the fin is zero and the end cooling Biot number at the tip of the fin is very large. This study will help in accurate analysis and design of heat sinks and passive devices for heat transfer enhancement for thermal and electronic systems.

**Keywords:** Thermal Management; Radiative-Convective fin, Diabatic tip, Thermal contact resistance; Magnetic field, Transient analysis.

## 1. Introduction

The resistance to flow of electrons in electrical circuit, short-circuit or spark-gap, wrong manufacturing or design, frictions, improper connections, prolonged systems operations under high temperature and improper design of the cooling systems are the sources of excessive generation of heat in electrical and electronics devices. Indisputably, such high and excessive internally generated heat has destructive effects such as thermal damage and runaway or burn off, *integrated circuits leakage*, break down and frying of solid-state electronics, degradation of constituents and components of the systems. Consequently, electrical and electronics systems are designed with effective passive and active cooling systems. However, due to relative low cost and weight-to-volume ratio coupled with miniaturization of electrical and electronics systems, fins are continuously employed (Figs. 1-2) as passive devices for the effective cooling and prevention of thermal damages in the systems.

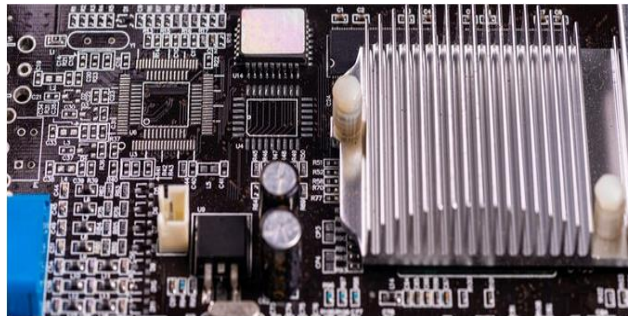


Fig. 1 Electronic circuit and cooling fins



(a)



(b)

Fig. 2 Cooling Fins in Electrical Machines (a) and Cooling Fins in Electric Power Transformers (b)

Research in passive heat transfer enhancement using fins has gained popularity due to applications in diverse systems (Kiwani and Al-Nimr, 2000; Das and Kundu, 2021). Modern electronics including microelectronics and embedded systems require improved processing power and electronic packaging. It is highlighted that for achievable improved processing power, the power density of semiconductors must double per Moore's principle (Moore, 2006). On the other side, several smaller electronic components are crammed up to achieve miniaturisation with improved processing power as an emerging electronic packaging and manufacturing trend. A key electronic packaging design concern in high processing power system to meet the operational threshold is excess heat generation (Oguntala *et al.*, 2019).

Considerable research effort in the literature highlights the impacts of various operational parameters including fin profile, porosity and material on the application potential of fins. Snider and Kraus (1986) addressed the fin optimum shaping issue, and Jany and Bejan (1985) analysed the optimal geometry for straight fins of temperature-dependent and variable conductivity. Kundu (2010) investigated the performance of optimised absorber-plate fin of variable conductivity to establish the dependency parameter on the fin performance and optimum design profile. Oguntala

et. al. (2018) investigated the thermal characteristic, stability and optimum design profile of rectangular fin to determine thermal stability criteria and optimum design parameters. Moitsheki (2011a, 2011b) highlighted the 1-D heat transfer in a triangular and hyperbolic fin with power-law temperature-dependent thermal conductivity and heat transport coefficient. Roy and Kundu (2018) investigated the effects of fin shapes on the thermal performance of microchannel heat sinks to establish the optimum conditions to achieve the least thermal resistance between the heatsink and fluid and maximise the heat transfer rate.

The findings of Kiwan and Al-Nimr (2000) on the effect of the porous medium to enhance heat transfer in fins, accelerated the popularity of porous fins. Porous fins offer the thermal advantage of effective surface area through which the fin transports heat to the working fluid. Sobamowo (2022) examined the Influence of fin surface tilt and magnetohydrodynamic effects on the thermal efficiency of porous fins. It is highlighted that porous fins are effective at low inclination angle, magnetic, porosity and radiative parameters values. Kiwan and Alzahrany (2007) discovered the critical threshold ratio value for effective and fluid thermal conductivities, above which the porous media behave as a fin, whilst below the threshold value behaves like an insulator. Kundu and Yook (2021) using a generalised analytical approach based on the differential transformation method (DTM) introduced the porosity factor in the natural convection term of porous fin analysis. Asadian et.al. (2017) using Galerkin and Akbari-Ganji's method investigated the heat transport through porous rectangular fins, whereas Deshamukhya *et al.* (2018) employed particle swarm optimisation to predict optimised key variables to maximise heat transport in rectangular porous fin. Shokouhmad et.al. (2018) investigated the effect of 2-D heat transport in porous fins of variable thermal conductivity of solid phase using finite difference method. Das and Kundu (2017) predicted the heat generation from the surface temperature of a porous fin.

The use of materials of various compositions, profiles and microstructure features has been identified to maximise heat transfer through fins (2019). Hatami and Ganji (2013) investigated the temperature distribution and heat transport of various selected materials such as Al, Cu, and ceramic (SiC, and Si<sub>3</sub>N<sub>4</sub>) in rectangular, triangular, convex and exponential profiles. Sobamowo *et al.* (2019) evaluated the fin performance of functionally graded material. Yasong and Benwen (2017) analysed the heat transport in fins using spectral element method.

Different solution methodologies including analytical, numerical, exact, semi-analytical, symbolic, experimental, programming and optimisation have been used to investigate the performance of fins for thermal enhancements in the literature (Sobamowo, 2016; Oguntala *et al.*, 2019, 2020; Roy *et al.*, 2015; Mosayebidorcheh *et al.*, 2014; Vahabzadeh *et al.*, 2015; Ghasemi *et al.*, 2014; Moradi *et al.*, 2014, Kundu and Lee, 2016; Jooma and Harley, 2017; Sobamowo *et al.*, 2022). These studies highlight the controlling models for the investigation of the thermal behaviour of fins as nonlinear. Most of these various solution methodologies offer different advantages and limitations including high computational complexity such as solutions with huge expressions and a large number of terms, limitations to linear problems, and time. The current solution approach is directed towards the use of various approximate analytical methods for symbolic solutions of nonlinear equations.

Moreover, the previous transient analyses of the extended surfaces have been done without proper considerations of the imperfect contact between the fin base and the prime surface. Also, the tip of the passive device has been assumed to be adiabatic. Therefore, the present work explores the impacts of thermal contact and diabatic tip on the transient nonlinear thermal performance of the longitudinal fin of temperature-dependent thermal conductivity subjected to the magnetic field under convective-radiative conditions using Generalized Integral Transform Techniques. The results of the developed approximate analytical solution are verified by the exact solution for the linear thermal model. The symbolic solutions are applied to investigate the effects of thermal model parameters on the performance of the longitudinal fin.

## 2. Formulation of the Problem

Given a porous rectangular fin under the influence of thermal convection and radiation (Fig. 3). The fin tip is diabatic and the base of the fin is not in perfect thermal contact with the prime surface. The fin is subjected to identical magnetic field applied in the perpendicular direction ( $y$ -direction) to the fin surface. The fin material is taken to be homogenous and isotropic with constant physical and thermal properties except the thermal conductivity.

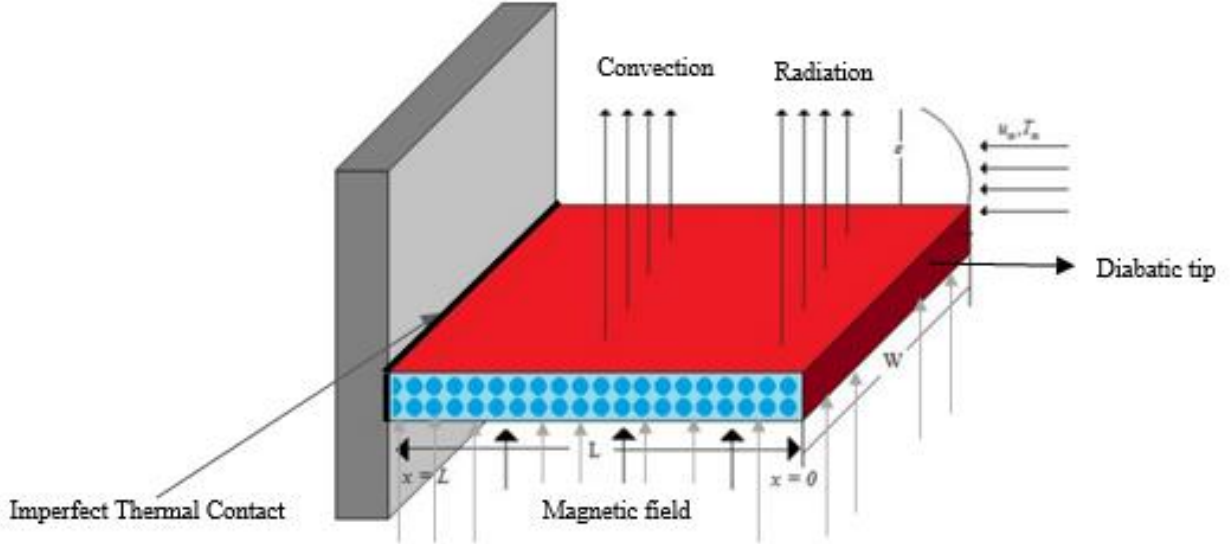


Fig. 3 Schematic of convective-radiative porous fin subjected to magnetic field

Thermal energy equation based on model assumptions is expressed as

$$\frac{\partial}{\partial \tilde{x}} \left( k(T^{**}) \frac{\partial T^{**}}{\partial \tilde{x}} \right) - \frac{\beta' c_p \rho g W K (T^{**} - T_\infty^*)^2}{A_{cr} v_f} - \frac{Ph}{A_{cr}} (T^{**} - T_\infty^*) - \frac{P \varepsilon \sigma}{A_{cr}} (T^{**4} - T_\infty^{*4}) - \frac{\mathbf{J}_c \times \mathbf{J}_c}{A_r \sigma_m} + q^m(T^{**}) = \rho c_p \frac{\partial T^{**}}{\partial \tilde{t}} \quad (1)$$

where  $J_c$ , the conduction current intensity is given as

$$\mathbf{J}_c = \sigma_m (E + V \times B)$$

It should be noted that

$$\frac{\mathbf{J}_c \times \mathbf{J}_c}{\sigma_m} = B_o^2 \sigma_m u^2 \quad (2)$$

Therefore, by substituting Eq. (2) into (1), we obtain

$$\frac{\partial}{\partial \tilde{x}} \left( k(T^{**}) \frac{\partial T^{**}}{\partial \tilde{x}} \right) - \frac{\beta' c_p \rho g W K (T^{**} - T_\infty^*)^2}{A_{cr} v_f} - \frac{Ph}{A_{cr}} (T^{**} - T_\infty^*) - \frac{P \varepsilon \sigma}{A_{cr}} (T^{**4} - T_\infty^{*4}) - \frac{B_o^2 \sigma_m u^2}{A_r} + q^m(T^{**}) = \rho c_p \frac{\partial T^{**}}{\partial \tilde{t}} \quad (3)$$

where thermal conductivity and the heat that is internally generated vary with temperature as a linear law

$$k_{eff}(T^{**}) = k_f \phi + k_s (1 - \phi) = k_{eff,b} [1 + \gamma(T^{**} - T_\infty^*)] \quad (4a)$$

$$q'''(T^{**}) = q_o''' (1 + \psi(T^{**} - T_\infty^*)) \quad (4b)$$

Introducing Eqs. (4) into Eq. (3), it gives

$$\begin{aligned} \frac{\partial}{\partial \tilde{x}} \left[ \left( 1 + \gamma(T^{**} - T_\infty^*) \right) \frac{\partial T^{**}}{\partial \tilde{x}} \right] - \frac{\beta' c_p \rho g W K (T^{**} - T_\infty^*)^2}{A_{cr} k_{eff,b} \nu_f} - \frac{Ph}{k_{eff,b} A_{cr}} (T^{**} - T_\infty^*) \\ - \frac{P \varepsilon \sigma}{k_{eff,b} A_{cr}} (T^{**4} - T_\infty^{*4}) - \frac{B_o^2 \sigma_m u^2}{k_{eff,b} A_r} + \frac{q_o'''}{k_{eff,b}} (1 + \psi(T^{**} - T_\infty^*)) = \frac{\rho c_p}{k_{eff,b}} \frac{\partial T^{**}}{\partial \tilde{t}} \end{aligned} \quad (5)$$

Initial condition is given as

$$\tilde{t} = 0, \quad 0 < \tilde{x} < L, \quad T^{**} = T_\infty^* \quad (6)$$

and boundary conditions expressed as

The boundary conditions for the thermal contact resistance and convective tip are given as

$$\tilde{t} > 0, \quad \text{when } \tilde{x} = 0, \quad -k(T^{**}) \frac{\partial T^{**}}{\partial \tilde{x}} = h_e (T^{**} - T_\infty^*) + \sigma \in (T^{**4} - T_\infty^{*4}) \quad (7)$$

$$\tilde{t} > 0, \quad \text{when } \tilde{x} = L, \quad -k(T^{**}) \frac{\partial T^{**}}{\partial \tilde{x}} = h_c (T_b - T^{**}) + \sigma \in (T^{**4} - T_a^{*4}) \quad (8)$$

Using the following dimensionless parameters of Eq. (9) in Eqs. (5)-(8)

$$\begin{aligned} X = \frac{\tilde{x}}{L}, \quad \theta = \frac{T^{**}}{T_L^*}, \quad \theta_\infty = \frac{T_\infty^*}{T_L^*}, \quad \tau = \frac{k_{eff,b} \tilde{t}}{\rho c_p L^2}, \quad Mc = \frac{PhL^2}{A_{cr} k_{eff,b}}, \quad Nr = \frac{\sigma \varepsilon P T_L^{*3} L^2}{A_{cr} k_{eff,b}}, \\ Sh = \frac{\rho c_p g W \beta' T_L^* K L^2}{A_{cr} \nu_f k_{eff,b}}, \quad Ha = \frac{\sigma_m B_o^2 u^2 L^2}{A_r k_{eff,b} T_L^*}, \quad Q = \frac{q_o''' L^2}{k_{eff,b} T_L^*}, \quad \beta = \gamma T_L^*, \quad \lambda = \psi T_L^* \end{aligned} \quad (9)$$

we arrived at the dimensionless forms of the governing as follows.

$$\begin{aligned} \frac{\partial}{\partial X} \left[ \left( 1 + \beta(\theta - \theta_\infty) \right) \frac{\partial \theta}{\partial X} \right] - Sh(\theta - \theta_\infty)^2 - Mc(\theta - \theta_\infty) - Nr(\theta^4 - \theta_\infty^4) \\ - Ha + Q(1 + \lambda(\theta - \theta_\infty)) = \frac{\partial \theta}{\partial \tau} \end{aligned} \quad (10)$$

Expansion Eq. (10), we have

$$\frac{\partial^2 \theta}{\partial X^2} + \beta \left( \frac{\partial \theta}{\partial X} \right)^2 + \beta \theta \frac{\partial^2 \theta}{\partial X^2} - \beta \theta_\infty \frac{\partial^2 \theta}{\partial X^2} - Sh\theta^2 + 2Sh\theta\theta_\infty - Sh\theta_\infty^2 - Mc\theta + Mc\theta_\infty - Nr\theta^4 + Nr\theta_\infty^4 - Ha + Q(1 + \lambda(\theta - \theta_\infty)) = \frac{\partial \theta}{\partial \tau} \quad (11)$$

and the dimensionless initial conditions is given as

$$\tau = 0, \quad \theta = 0, \quad 0 \leq X \leq 1 \quad (12)$$

The dimensionless boundary conditions are

$$\tau > 0, \text{ when } X = 0, \quad (1 + \beta\theta) \frac{d\theta}{dX} = -Bi\theta \quad (13)$$

$$\tau > 0, \text{ when } X = 1, \quad (1 + \beta\theta) \frac{d\theta}{dX} = -Bi_c(1 - \theta) \quad (14)$$

### 3. The Hybrid Analytical-Numerical Solutions for the Nonlinear Thermal Problems

Indisputably, the developed nonlinear and linear thermal models can easily be solved numerically and analytically, respectively. However, the computational methods are approximate methods with inherent high computational cost and time. The approximate solutions involve power series with the rigorous solution procedures and large number of terms are not convenient for use in practice. Therefore, the obvious advantages of generating non-power series analytical solutions to the nonlinear problems are very much important and this is given in the present study. Such non-power series solutions allow effective thermal predictions of the extended surface over a large domain and time. Also, the non-power series solutions reduce the complex mathematical analysis that gives analytic expressions involving large number terms, high computational cost and time. Therefore, it very important to find non-power series solutions to the thermal problems. Moreover, an excursion into literature shows the rare application of generalized integral transform technique (GITT) to thermal analysis of fins. Such a hybrid analytical-numerical solution will provide better physical insights into the importance of thermo-physical parameters than a total numerical method. In the generation of the analytical solutions to differential equations, the practical significance of transform methods facilitates observation of great many properties and hidden views, of both mathematical and physical interest, which are not yet well known and have not met with proper appreciation.

#### 3.1. Generalized Integral Transform Technique

GITT is a hybrid analytical-numerical solution that is based on eigenfunctions expansion of a Sturm-Liouville problem from a partial differential equation (Mikhailov and Ozisik, 1984; Cotta, 1990, Cotta, 1994; Cotta *et al.*, 2018, Cotta *et al.*, 2019, Cotta *et al.*, 2020; Knupp *et al.*, 2015, and Knupp *et al.*, 2020). With the aid of an integral transform pair and a Sturm-Liouville eigenvalue problem, the developed partial differential equation can be converted into a coupled system of ordinary differential equations. Unfortunately, the system of the differential equations does not have a general method that will always provide analytical solutions. Consequently, a readily available recourse is a numerical technique to solve the set of the equations. Therefore, the generalized integral transform technique is often referred to as a hybrid analytical-numerical method. In the course of providing the need solution to the system of the differential equations with the GITT, the potential solution is obtained by applying the inverse function of the transformed pair which gives an eigenfunction expansion that must be truncated to obtain the desired convergence of the solution.

It is recommended to homogenize the boundary conditions using a simple filter defined as:

$$\theta(X, \tau) = \Theta(X, \tau) + 1 \tag{15}$$

where  $\Theta(X, \tau)$  is the filtered potential. The simple filter enhances the computational efficiency of the solution. Also, it helps to reduce the numbers of terms in the eigenfunction expansion,

Substituting Eq. (15) into Eqs. (11)-(14),

$$\begin{aligned} \frac{\partial^2 \Theta}{\partial X^2} + \beta(\Theta + 1) \frac{\partial^2 \Theta}{\partial X^2} + \beta \left( \frac{\partial \Theta}{\partial X} \right)^2 - \beta \theta_\infty \frac{\partial^2 \Theta}{\partial X^2} - Sh(\Theta + 1)^2 + 2Sh\theta_\infty(\Theta + 1) - Sh\theta_\infty^2 \\ - Mc(\Theta + 1) + Mc\theta_\infty - Nr(\Theta + 1)^4 + Nr\theta_\infty^4 - Ha + Q(1 + \lambda((\Theta + 1) - \theta_\infty)) = \frac{\partial \Theta}{\partial \tau} \end{aligned} \tag{16}$$

and for the initial

$$\tau = 0, \quad \Theta = -1, \quad 0 \leq X \leq 1 \tag{17}$$

as well as the boundary conditions

$$\tau > 0, \text{ when } X = 0, \quad (1 + \beta(\Theta + 1)) \frac{d\Theta}{dX} = -Bi(\Theta + 1) \tag{18}$$

$$\tau > 0, \text{ when } X = 1, \quad (1 + \beta(\Theta + 1)) \frac{d\Theta}{dX} = Bi_c \Theta \tag{19}$$

After expansion and collection of like terms in Eq. (15), we arrived at

$$\begin{aligned} \frac{\partial^2 \Theta}{\partial X^2} + \beta(\Theta + 1) \frac{\partial^2 \Theta}{\partial X^2} + \beta \left( \frac{\partial \Theta}{\partial X} \right)^2 - \beta \theta_\infty \frac{\partial^2 \Theta}{\partial X^2} - Nr\Theta^4 - 4Nr\Theta^3 - 6Nr\Theta^2 - Sh\Theta^2 + 2Sh\theta_\infty\Theta - 2Sh\Theta \\ - Mc\Theta + Q\lambda\Theta - 4Nr\Theta - Sh\theta_\infty^2 + 2Sh\theta_\infty - Sh - Mc + Mc\theta_\infty + Nr\theta_\infty^4 - Ha + Q + Q\lambda - Q\lambda\theta_\infty - Nr = \frac{\partial \Theta}{\partial \tau} \end{aligned} \tag{20}$$

Having properly defined the filtered problem, we can now easily apply GITT formalism via a transform and inverse pair as follows:

$$\text{Transform: } \bar{\Theta}_i(\tau) = \int_0^1 \Theta(X, \tau) \tilde{\psi}_i(X) dX \tag{21a}$$

$$\text{Inverse: } \Theta(X, \tau) = \sum_i \tilde{\psi}_i(X) \bar{\Theta}_i(\tau) \tag{21b}$$

The normalized eigenfunctions is written as

$$\bar{\psi}_i(X) = \frac{\psi_i(X)}{\sqrt{N_i}} \tag{22}$$

Following the filtering process,  $\Theta(X, \tau)$  can be expanded in a series of eigenfunctions:

$$\Theta(X, \tau) = \sum_i \frac{\psi_i(X) \bar{\Theta}_i(\tau)}{\sqrt{N_i}} \tag{23}$$

where the orthogonal eigenfunctions,  $\psi_i$  satisfies

$$\int_0^1 \psi_i(X) \psi_j(X) dX = \delta_{i,j} N_i = \delta_{i,j} N_j \tag{24}$$

where  $\delta_{i,j}$  and  $N_i$  represent the Kronecker delta

The norms of the eigenfunctions are given as

$$N_i = \int_0^1 \tilde{\psi}_i^2(X) dX \tag{25}$$

Using the Sturm-Liouville problem solution, we can easily obtain the eigenfunctions  $\psi_i(X)$ . For example, adopting the simplest eigenvalue problem,

$$\frac{\partial^2 \psi_i}{\partial X^2} + \mu_i^2 \psi_i = 0 \tag{26}$$

With the boundary conditions

$$\psi_i = 0 \text{ at } X = 0 \tag{27}$$

$$\frac{\partial \psi_i}{\partial X} = 0 \text{ at } X = 1$$

Which gives the solution

$$\psi_i(X) = \sin \left[ \left( \frac{2i-1}{2} \right) \pi X \right], \quad i = 1, 2, 3, \dots \tag{26}$$

With the norm given as

$$N_i = \frac{1}{2} \tag{27}$$

For further reading on the solutions of the Sturm-Liouville problem under different boundary conditions, the reader is referred to Mikhailov and Özisik (1984) for the solution of Eq. (24)

Now using the operator  $\int_0^1 (\square) \tilde{\psi}_i(X) dX$  on Eq. (18) and the inversion formulae in Eq.(19b), the following transformed system of initial-value problem and its corresponding initial condition are obtained:

$$\begin{aligned} \sum_{j=1}^{\infty} \frac{\partial \bar{\Theta}_j(\tau)}{\partial \tau} A_{i,j} &= \sum_{j=1}^{\infty} \sum_{k=1}^{\infty} \bar{\Theta}_j(\tau) \bar{\Theta}_k(\tau) B_{i,j,k} + \sum_{j=1}^{\infty} \sum_{k=1}^{\infty} \sum_{l=1}^{\infty} \sum_{m=1}^{\infty} \bar{\Theta}_j(\tau) \bar{\Theta}_k(\tau) \bar{\Theta}_l(\tau) \bar{\Theta}_m(\tau) C_{i,j,k,l,m} \\ &+ \sum_{j=1}^{\infty} \sum_{k=1}^{\infty} \sum_{l=1}^{\infty} \bar{\Theta}_j(\tau) \bar{\Theta}_k(\tau) \bar{\Theta}_l(\tau) D_{i,j,k,l} + \sum_{j=1}^{\infty} \sum_{k=1}^{\infty} \bar{\Theta}_j(\tau) \bar{\Theta}_k(\tau) E_{i,j,k} + \sum_{j=1}^{\infty} \bar{\Theta}_j(\tau) F_{i,j} + D_i \end{aligned} \tag{28}$$

with the initial condition as

$$\bar{\Theta}_i(0) = -\int_0^1 \tilde{\psi}_i(X) dX \tag{29}$$

where

$$A_{i,j} = \int_0^1 \tilde{\psi}_i(X) \tilde{\psi}_j(X) dX$$

$$B_{i,j,k} = \beta \left[ \int_0^1 \frac{\partial \tilde{\psi}_j(X)}{\partial X} \frac{\partial \tilde{\psi}_k(X)}{\partial X} \tilde{\psi}_i(X) dX - \mu_k^2 \int_0^1 \tilde{\psi}_k(X) \tilde{\psi}_j(X) \tilde{\psi}_i(X) dX \right]$$

$$C_{i,j,k,l,m} = -Nr \int_0^1 \tilde{\psi}_m(X) \tilde{\psi}_l(X) \tilde{\psi}_k(X) \tilde{\psi}_j(X) \tilde{\psi}_i(X) dX$$

$$D_{i,j,k,l} = -4Nr \int_0^1 \tilde{\psi}_l(X) \tilde{\psi}_k(X) \tilde{\psi}_j(X) \tilde{\psi}_i(X) dX$$

$$E_{i,j,k} = -(6Nr + Sh) \int_0^1 \tilde{\psi}_k(X) \tilde{\psi}_j(X) \tilde{\psi}_i(X) dX$$

$$F_{i,j} = -\left[ (1 + \beta - \beta\theta_\infty) \mu_k^2 \int_0^1 \tilde{\psi}_j(X) \tilde{\psi}_i(X) dX + (2Sh\theta_\infty\Theta - 2Sh\Theta - Mc + Q\lambda - 4Nr) \int_0^1 \tilde{\psi}_j(X) \tilde{\psi}_i(X) dX \right]$$

$$G_i = -\left( Sh\theta_\infty^2 - 2Sh\theta_\infty + Sh + Mc - Mc\theta_\infty - Nr\theta_\infty^4 + Ha - Q - Q\lambda + Q\lambda\theta_\infty + Nr \right) \int_0^1 \tilde{\psi}_i(X) dX$$

There is no analytical solution for the system of nonlinear equations in Eq. (10). Therefore, a necessary recourse is numerical method. With the aid of *NDSolve* routine from Wolfram Mathematica software, numerical method is applied to solve the system of nonlinear equations which is being truncated to an order N (which was chosen for the desired convergence and accuracy of the solution). The software gives the required solutions to the system of the nonlinear ODEs with predetermined controls of the relative and absolute errors.

Having found  $\bar{\Theta}_i(\tau)$  numerically, using the inversion formulae in Eq. (19b), one can find  $\Theta(X, \tau)$  as

$$\Theta(X, \tau) = \sum_i^N \tilde{\psi}_i(X) \bar{\Theta}_i(\tau) \tag{30}$$

From Eq. (14), the required dimensionless temperature  $\theta(X, \tau)$  can be expressed as

$$\theta(X, \tau) = 1 + \sum_i^N \tilde{\psi}_i(X) \bar{\Theta}_i(\tau) \tag{31}$$

To validate the GITT solutions, the numerical solution was provided for the nonlinear model using Crank-Nicolson finite different method due to its unconditional mathematical stability. The solution is presented as

$$\begin{aligned} & \left( \frac{\theta_{i+1}^{n+1} - 2\theta_i^{n+1} + \theta_{i-1}^{n+1} + \theta_{i+1}^n - 2\theta_i^n + \theta_{i-1}^n}{2\Delta^2 X} \right) + \beta(\theta_i^n) \left( \frac{\theta_{i+1}^{n+1} - 2\theta_i^{n+1} + \theta_{i-1}^{n+1} + \theta_{i+1}^n - 2\theta_i^n + \theta_{i-1}^n}{2\Delta^2 X} \right) \\ & + \beta \left( \frac{\theta_{i+1}^{n+1} - \theta_{i-1}^{n+1} + \theta_{i+1}^n - \theta_{i-1}^n}{4\Delta X} \right)^2 - \beta\theta_\infty \left( \frac{\theta_{i+1}^{n+1} - 2\theta_i^{n+1} + \theta_{i-1}^{n+1} + \theta_{i+1}^n - 2\theta_i^n + \theta_{i-1}^n}{2\Delta^2 X} \right) - Sh(\theta_i^n)^2 \\ & + 2Sh\theta_i^n\theta_\infty - Sh\theta_\infty^2 - Mc\theta_i^n - Nr(\theta_i^n)^4 - Ha + Mc\theta_\infty + Nr\theta_\infty^4 + Q(1 + \lambda(\theta_i^n - \theta_\infty)) = \left( \frac{\theta_i^{n+1} - \theta_i^n}{\Delta\tau} \right) \end{aligned} \tag{32}$$

The FDM of the initial condition is

$$\theta_i^o = 0, \quad (33)$$

and FDM of boundary conditions is

$$(1 + \beta\theta_M^n) \left( \frac{\theta_{M+1}^n - \theta_{M-1}^n}{2\Delta X} \right) = -Bi\theta_M^n \Rightarrow \theta_{M+1}^n = \theta_{M-1}^n - \frac{2\Delta X Bi \theta_M^n}{(1 + \beta\theta_M^n)} \quad (34)$$

$$(1 + \beta\theta_M^n) \left( \frac{\theta_{M+1}^n - \theta_{M-1}^n}{2\Delta X} \right) = Bi(\theta_M^n - 1) \Rightarrow \theta_{M+1}^n = \theta_{M-1}^n + \frac{2\Delta X Bi}{(1 + \beta\theta_M^n)} (\theta_M^n - 1) \quad (35)$$

#### 4. Results and Discussion

The solutions of GITT are developed and the results of the parametric studies are shown in Figs. 4-22. However, Table 1 illustrate the comparison between finite difference method (FDM) and GITT results for the nonlinear thermal models

Table 1: Comparison of results

X	FDM	GITT
0.0000	0.9581	0.9581
0.2000	0.9597	0.9597
0.4000	0.9647	0.9647
0.6000	0.9730	0.9730
0.8000	0.9846	0.9846
1.0000	1.0000	1.0000

Figures 4 – 20 display the impact of convection-conduction, radiation-conduction, magnetic field, contact resistance and diabatic parameters on the dimensionless transient temperature profiles of the fin.

Figures 4, 5 and 6 is drawn to investigate the impact of conduction-convection on heat transport through the longitudinal fin while Figures 7 and 8 explores the roles of conduction-radiation parameters on the dimensionless thermal performance of the passive device. It is noticed that the temperature of the fin decreases as the convection-conduction and radiation-conduction parameters increase. This depicts an increase in the surface heat loss of the fin as the heat transfer coefficient increases and invariably increased heat dissipation capability.

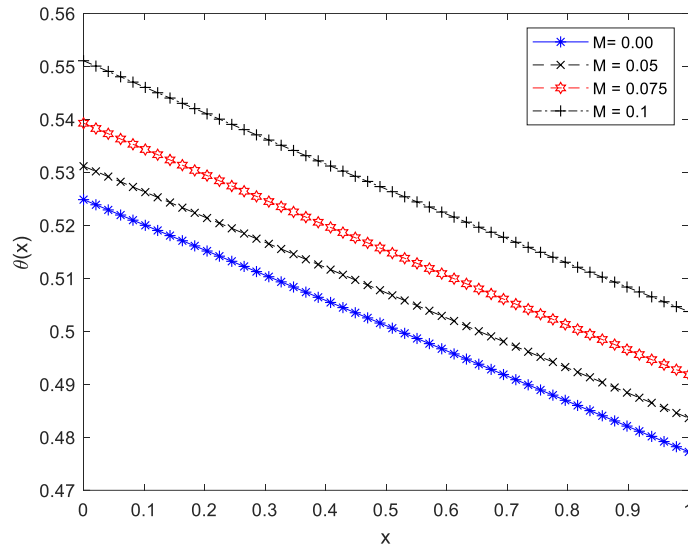


Fig. 4 Impact of convective parameter on the dimensionless temperature distribution in the fin when  $Nr=0.1$

The increase in the heat transfer coefficient significantly improves the heat transport from the base of the passive device and the surrounding fluid as the fin surface convects more heat away from the fin surface, which decrease the temperature distribution of the fin and improve the heat transport in the extended surface. For the conduction-radiative influence, the decrease in the fin temperature is due to increased heat transport from the fin surface via thermal radiation, which subsequently increases the intensity of the radiative cooling.

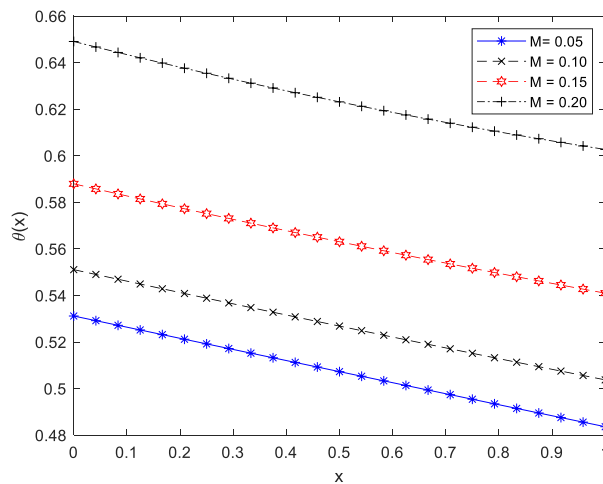


Fig. 5 Impact of convective parameter on the dimensionless temperature distribution in the fin when  $Nr=0.2$

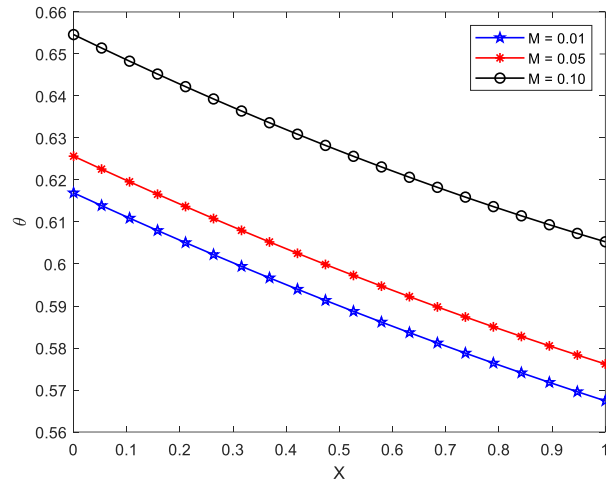


Fig. 6 Impact of convective parameter on the dimensionless temperature distribution in the fin when  $Nr=0.3$

The impact of magnetic field parameters on the dimensionless temperature distribution in the conductive-radiative extended surface is shown in Fig. 9. From the illustration, when the magnetic field parameter is augmented, the dimensionless local temperature in the conductive-radiative device is enhanced. The increase in the magnetic parameter increases the Lorentz force which provides resistive force to oppose the motion of the fin working fluid and consequently, the fin temperature decreases.

On the issue of contact resistance, the imperfect thermal contact, the reason for the response is because, as the conduction-convection, conduction-radiation and magnetic field parameters increase, the convective heat in the gap between the prime surface and fin base increases. This convective heat which is of higher heat transfer coefficient than that of the fin surface and tip, is mainly absorbed by the fin through its base. Consequently, more heat is gained from the base of the fin than to the heat loss from the surface and the tip of the fin. Therefore, as the conductive-convective, conductive-radiative and magnetic field parameters increase, the dimensionless temperature in the fin also increases.

However, if the assumption of perfect thermal contact between the prime surface and the fin base prevails, it will be that as the convection-conduction, radiation-conduction and magnetic field parameters are augmented, the dimensionless temperature in the fin will depreciate. As a consequence, there is an increase in the heat loss from the surface of the fin. As a consequent, surface temperature of the fin drops (the fin thermal profile falls) and the rate of heat transfer from the fin increases as the convective, radiative and magnetic field parameters increase. It should be noted that the low value of the convective parameter and radiative,  $M$  and  $Nr$  implies a relatively thick and short fin of very high thermal conductivity while a high value of the convective and radiative parameters indicates a relatively thin and long fin of a very low thermal conductivity. Therefore, under the condition of perfect thermal contact between the prime surface and the base of the fin, the rate of heat transfer from the extended surface and the fin thermal efficiency are favoured at low these thermo-magneto-geometric parameters, i.e. a relatively thick and short fin with a high thermal conductivity.

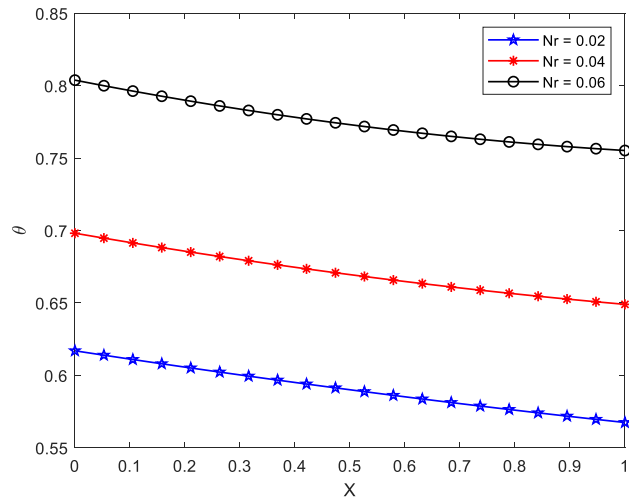


Fig. 7 Effect of radiative parameter on the dimensionless temperature distribution in a convective-radiative fin when  $M=1.0$

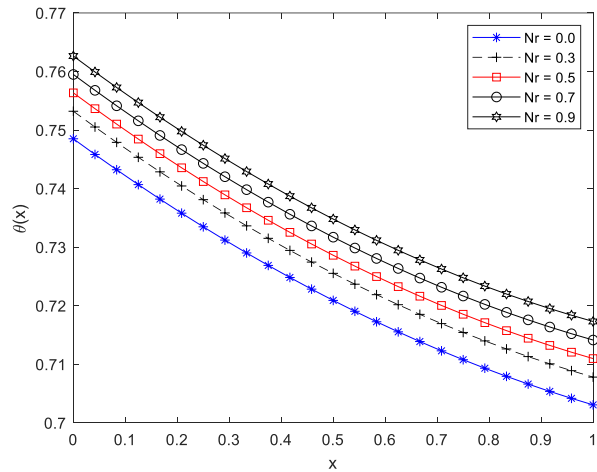


Fig. 8 Effect of radiative number on the dimensionless temperature distribution in a convective-radiative fin when  $M=0.2$

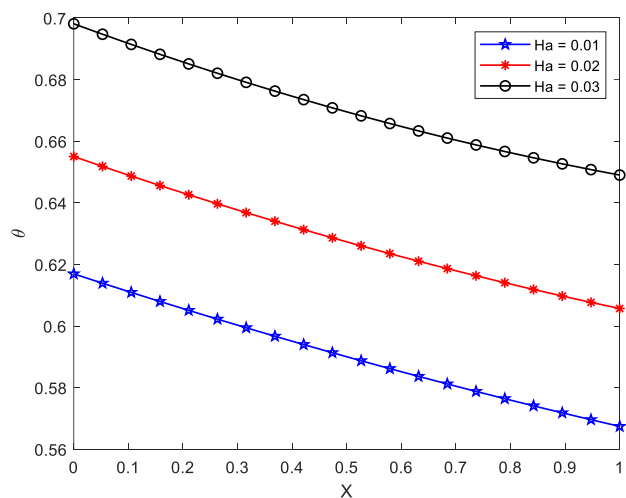


Fig. 9 Effect of Hartmann (magnetic field) parameter on the dimensionless temperature distribution in a convective-radiative fin

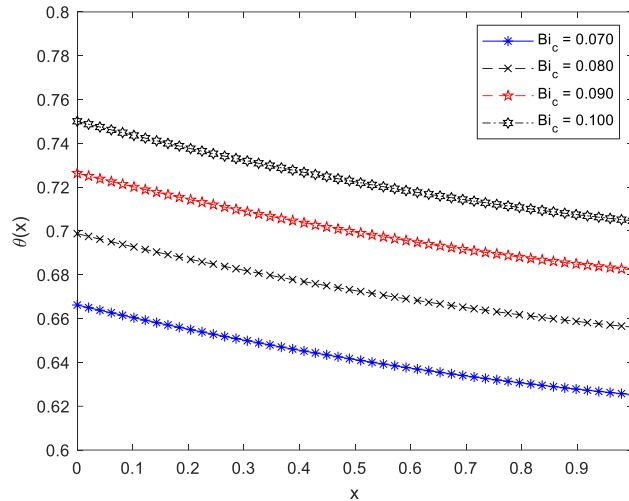


Fig. 10 Effect of thermal contact Biot number on the dimensionless temperature distribution in a convective-radiative fin when  $Nr=0.1$

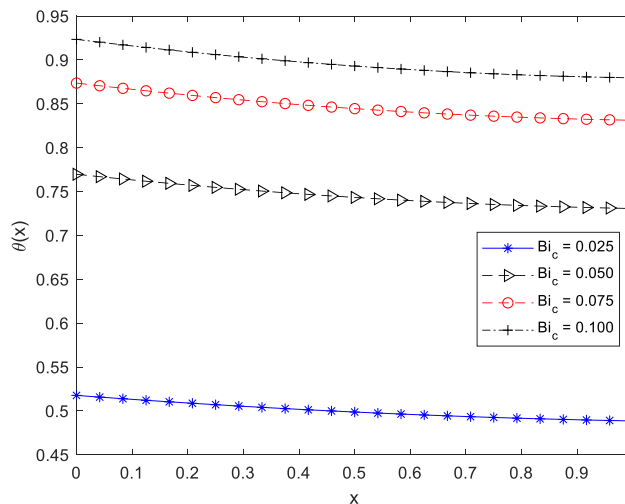


Fig. 11 Effect of thermal contact Biot number on the dimensionless temperature distribution in a convective-radiative fin when  $Nr=0.3$

Figs. 10 and 11 show the effect of thermal contact Biot number on the nondimensional temperature of the porous fin at the point where the radiative-convecting fin joins with the prime surface while Fig. 12 presents the effect of end cooling Biot number on a conductive- fin at the tip of the fin. The fin base and tip Biot numbers have significant effect on the fin temperature. This happens at the comparably low values of the conductive-convective, conductive-radiative, magnetic field and thermal conductivity parameters A further analysis revealed that at comparably high values of the conductive-convective, conductive-radiative and magnetic field parameters, the variations in the Biot numbers do not have significant effect on the fin temperature. However, when the tip of the fin is assumed insulated or the end cooling Biot number is zero, there are significant variations in the temperature of the conductive-radiative fin.

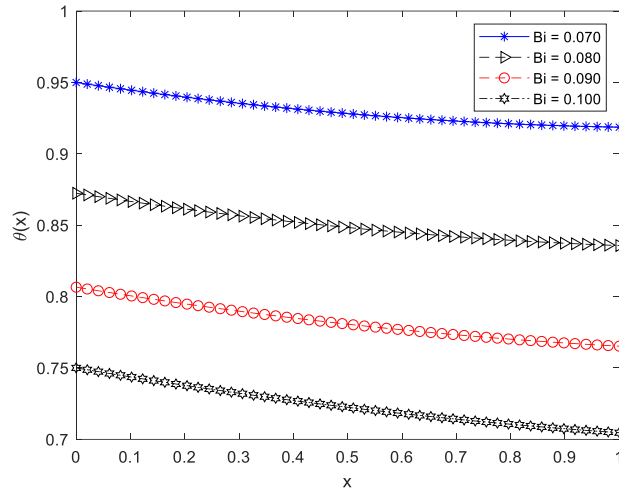


Fig. 12 Effect of end cooling Biot number on the dimensionless temperature distribution in a convective-radiative fin

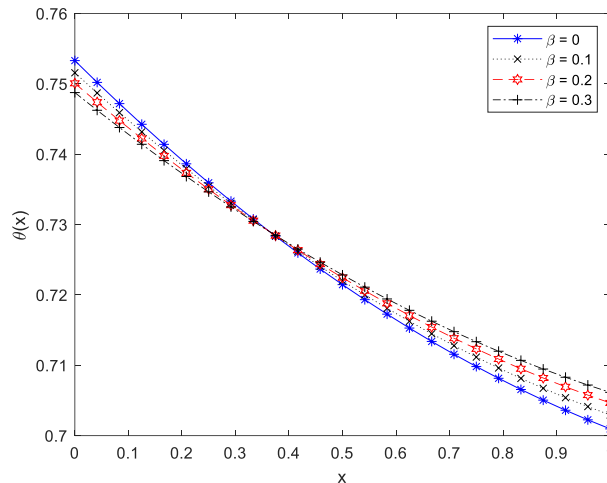


Fig. 13 Effect of nonlinear thermal conductivity parameter on the dimensionless temperature distribution in a convective-radiative fin

Fig. 13 presents the effects of thermal conductivity parameter,  $\beta$  on the dimensionless temperature distribution in the fin. It is shown that the fin temperature is indirectly and directly proportional to the fin thermal conductivity from  $0 < X < 0.35$  and  $0.35 < X < 1.00$ , respectively. Physically speaking, when the thermal conductivity parameter is amplified which results in a decrease in the local temperature of the fin within the range  $0 < X < 0.35$ . However, when the thermal conductivity parameter is magnified, there is a decrease in the local dimensionless temperature of the fin within the range  $0.35 < X < 1.00$ .

This behaviour is as depicted in the figure is not general behaviour but it is based on the respective values of thermal contact Biot number (which depicts the extent of thermal contact) at the fin base and the fin tip Biot number. In order to establish this fact, effect of the nonlinear thermal conductivity when thermal contact Biot number at the base of the fin and the end cooling Biot number at the tip of the fin are 0 and 10, respectively as shown in Fig. 14. It is shown that when the thermal conductivity parameter is amplified, there is an increase in the local dimensionless temperature of the fin as shown in the figure. It is further observed that the temperature of the fin-tip amplifies as the thermal conductivity parameter magnifies.

The impact of thermo-geometric or conductive-convective parameter on the dimensionless temperature distribution in the conductive and non-radiative fin is shown in Figs. 15 and 16 while Fig. 17 shows the effect of thermal contact Biot number on a fin at the point where the conductive and non-radiative fin joins with the prime surface. Fig. 18 presents the effect of end cooling Biot number on a conductive and non-radiative fin at the tip of the fin.

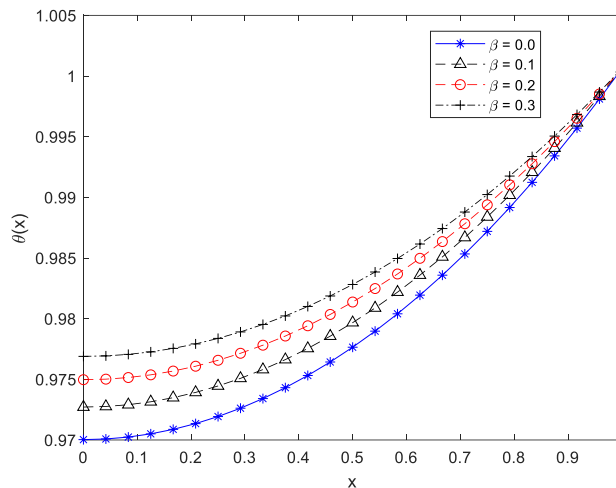


Fig. 14 Effect of nonlinear thermal conductivity parameter on the dimensionless temperature distribution in a convective-radiative fin  $Bi=0$  and  $Bi_c=10$ (the large value is for approximately perfect thermal contact)

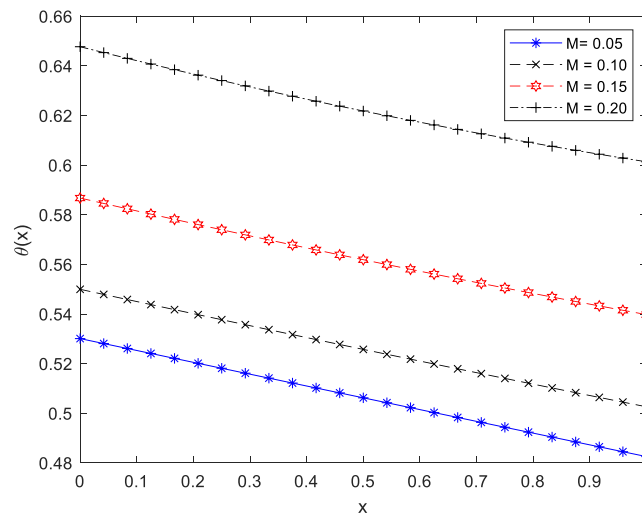


Fig. 15 Effect of convective parameter on the dimensionless temperature distribution in a convective and non-radiating fin when  $Bi_c=0.1$

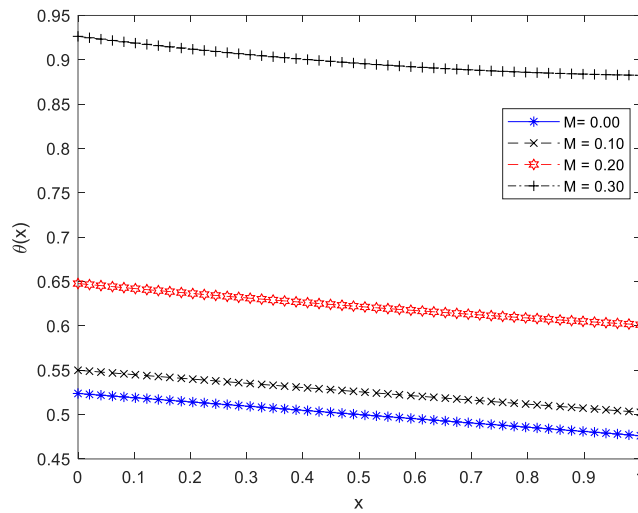


Fig. 16 Effect of convective parameter on the dimensionless temperature distribution in a convective and non-radiative fin when  $Bi_c=0.05$

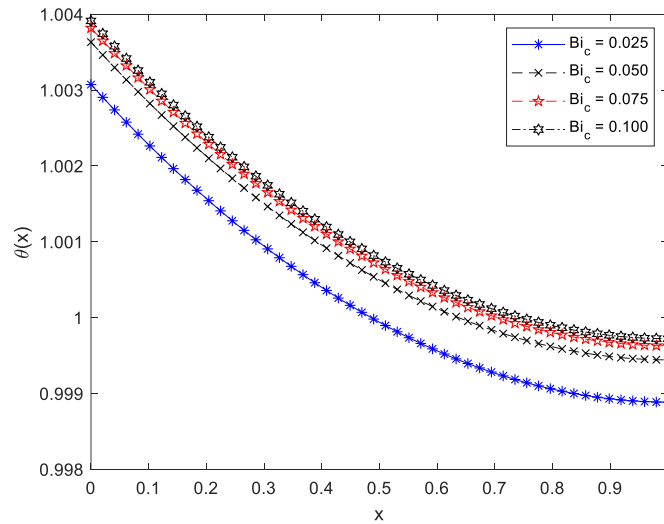


Fig. 17 Effect of thermal contact Biot number on the dimensionless temperature distribution in a convective and non-radiative fin

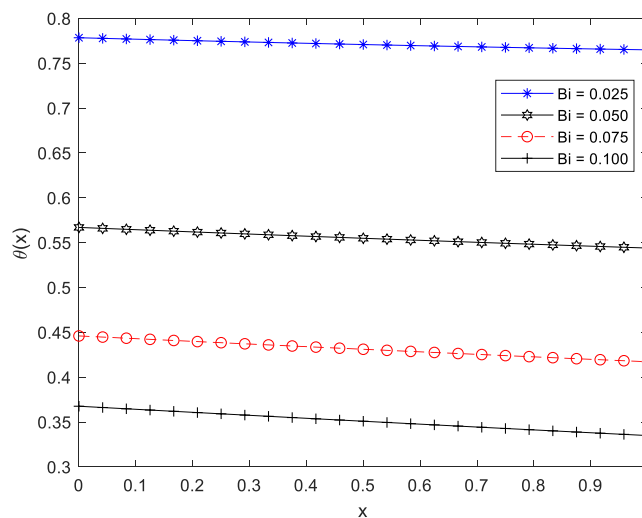


Fig. 18 Effect of end cooling Biot number on the dimensionless temperature distribution in a convective and non-radiative fin

The impact of conductivity  $\beta$ , on the dimensionless transient thermal behaviour of extended surface with porosity is illustrated in Figs. 19 and 20. It is shown that the conductive and non-radiative fin temperature is indirectly and directly proportional to the fin conductivity from  $0 < X < 0.35$  and  $0.35 < X < 1.00$ , respectively. The increase in both conductivity and its gradient leads to a rise in the local temperature of the fin. The heightened local temperature of the fin results in an increase in heat transport in the fin, which consequently reduce heat dissipation capability of the fin. It is worth noting that high conductivity materials tend to store more heat than dissipate it as compared to a material of low conductivity materials that dissipates more heat. Therefore, for increased heat dissipation as required as in high power electronics and embedded systems, relatively low conductivity materials are effective for thermal enhancement.

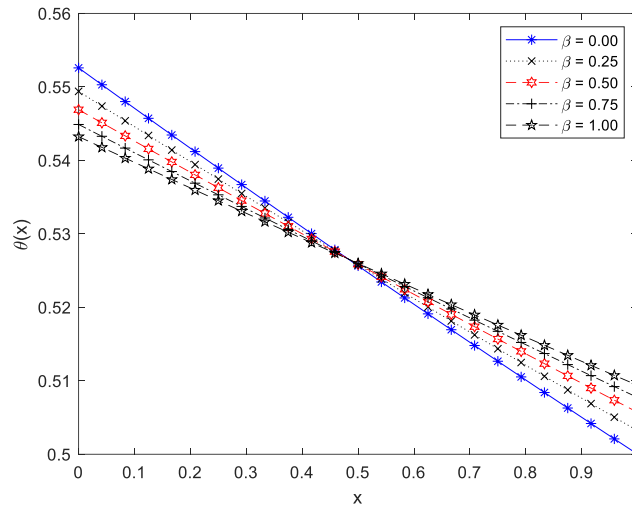


Fig. 19 Effect of nonlinear thermal conductivity parameter on the dimensionless temperature distribution in a convective and non-radiative fin

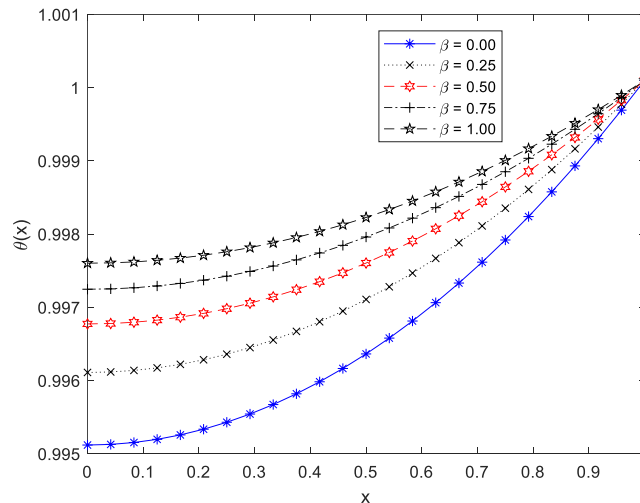


Fig. 20 Effect of nonlinear thermal conductivity parameter on the dimensionless temperature distribution in a convective-radiative fin  $Bi=0$  and  $Bic=10$  (the large value is for approximately for perfect thermal contact)

In order to establish this fact, effect of the nonlinear conductivity parameter when thermal contact Biot number at the base of the conductive and non-radiative fin and the end cooling Biot number at the tip of the fin are 0 and 10, respectively as shown in Fig. 20. As shown in the previous Fig. 20, when the conductivity parameter is amplified, there is an increase in the local temperature of the fin. It is also observed that the temperature of the fin-tip amplifies as the conductivity parameter magnifies. The non-radiating effect does not change the thermal behaviour of the fin as the same effects are recorded in all the figures.

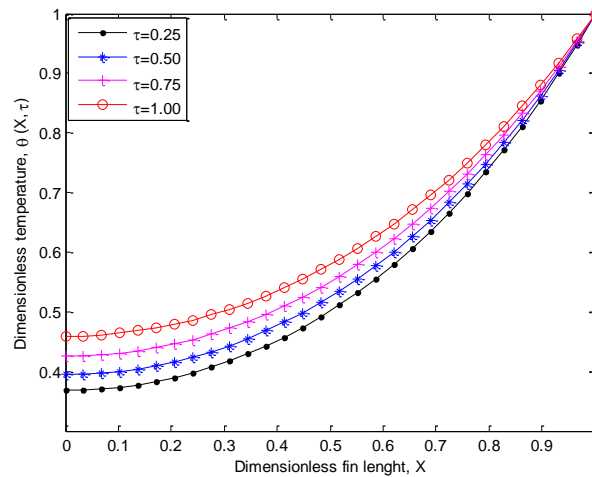


Figure 21. Impact of time on the fin thermal distribution

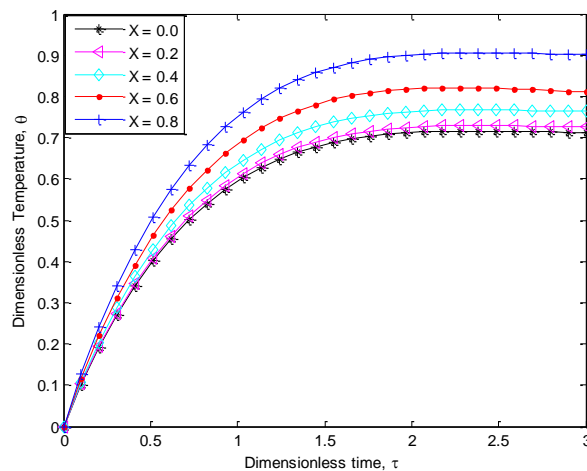


Figure 22. Temperature history in the fin at various locations in the fin

Fig. 21 demonstrates the fin temperature profiles at different timeframes, whilst the temperature evolution at various positions in the fin is shown in Figure 22. The figures highlight that at different fin positions, an increased temperature is experienced with increase in time. The time periods in the solution reveal that the transient solution approaches a steady state as the tip temperature increases over time.

## 5. Conclusion

In this paper, the effects of thermal contact resistance at the fin base, a convecting-radiative (end cooling) tip and magnetic field on the thermal performance of a convecting and radiating fin with temperature-variant thermal conductivity have been numerically investigated with the aid of generalized integral transform techniques. The parametric studies reveal the following:

- i. The dimensionless local temperature in the radiative-conductive porous fin is augmented when the conductive-convective, conductive-radiative and magnetic field parameters are amplified.
- ii. With the assumption of perfect thermal contact between the prime surface and the base of the fin, the dimensionless temperature in the passive device depreciates as the convective-conductive, radiative-conductive and magnetic field parameters appreciate.
- iii. The fin dimensionless local temperature is significantly affected by the Biot numbers under the comparably low values of the convective-conductive, radiative-conductive, magnetic field and thermal conductivity parameters
- iv. At comparably high values of the convective-conductive, radiative-conductive and magnetic field parameters, the variations in the Biot numbers do not significantly affect the temperature of the fin.
- v. When the tip of the fin is assumed adiabatic or the end cooling Biot number is zero, there are significant variations in the temperature of the radiative-conductive porous fin.
- vi. The effects of the fin conductivity parameter along the fin length depend on the respective values of thermal contact Biot number at the base of the fin and the end cooling Biot number at the tip of the fin.
- vii. When the conductivity parameter is amplified, the fin dimensionless temperature increases when thermal contact Biot number at the base of the fin and the end cooling Biot number at the tip of the fin are 0 and 10 (or very large), respectively.
- viii. When conductivity parameter is increased, the fin tip temperature is magnified.
- ix. For different positions in the fin, the temperature increases with an increase in time. Consequently, the time histories of the solution depict the transient solution converging to a steady state as the fin tip temperature increases with time progression.

The study provides high accurate prediction of thermal performance of longitudinal fins and a good platform for the effective design of extended surfaces in thermal and power electronics.

## Nomenclature

$A_{cr}$	Cross-sectional area of fin, [ $m^2$ ]
$A_r$	Ratio of surface area to the cross-sectional area
$A_{cr}$	Cross-sectional area of fin, [ $m^2$ ]
$A_r$	Ratio of surface area to the cross-sectional area
$T$	Fin Temperature, [ $K$ ]
$T_L$	Temperature at fin base, [ $K$ ]
$T_\infty$	Ambient temperature, [ $K$ ]
$k$	Thermal conductivity of fin, [ $Wm^{-1}K^{-1}$ ]
$k_b$	Thermal conductivity at fin base, [ $Wm^{-1}K^{-1}$ ]
$J_c$	Conduction current intensity, [ $A$ ]
$J$	Total current intensity, [ $A$ ]
$x$	Axial distance of Fin, [ $m$ ]
$L$	Fin length, [ $m$ ]
$P$	Fin perimeter, [ $m$ ]
$B_o$	Magnitude of magnetic field, [ $\Omega^{1/2}kg^{1/2}m^{-1}s^{1/2}$ ] or $T$
$t$	Time, [ $sec$ ]

$E$	External electric field, [ $V \cdot m^{-1}$ ]
$u$	Axial velocity, $m/sec$ [ $m \cdot sec^{-1}$ ]
$c_p$	Specific heat capacity, [ $J \cdot kg^{-1} \cdot K^{-1}$ ]
$V$	Macroscopic velocity of electrons
$h$	Heat transmission coefficient, [ $W \cdot m^{-2} \cdot K^{-1}$ ]
$\chi$	Dimensionless fin length
$M_c$	Dimensionless convective parameter
$N_r$	Dimensionless radiation parameter
$Ha$	Hartman number
$Bi$	Biot number

### Greek Symbols

$\beta$	Coefficient of nonlinear thermal conductivity, [ ]
$\varepsilon$	Emissivity of Fin material
$\delta$	Fin thickness, [ $m$ ]
$\tau$	Dimensionless time
$\theta$	Dimensionless temperature
$\theta_L$	Dimensionless temperature at fin base
$\rho$	Density of Fin [ $kg \cdot m^{-3}$ ]
$\sigma$	Stefan Boltzmann constant, [ $W \cdot m^{-2} \cdot K^{-4}$ ]
$\sigma_m$	Electric conductivity, [ $\Omega^{-1} \cdot m^{-1} \cdot K^{-1}$ ]
$\gamma$	<b>Dimensional</b> nonlinear thermal conductivity coefficient [ $K^{-1}$ ]

## References

- Asadian, H., Zaretabar, M., Ganji, D. D., Gorji-Bandpy, M., and Sohrabi, S. (2017). Investigation of Heat Transfer in Rectangular Porous Fins with Temperature-Dependent Internal Heat Generation by Galerkin's Method (GM) and Akbari-Ganji's Method (AGM)," *International Journal of Applied and Computational Mathematics*, 3(4), 2987-3000.
- Cotta, R. M, Lisboa, K. M., Curi, M. F., Balabani, S. Quaresma, J.N.N, Perez-Guerrero, J. S., Macêdo, E. N., Amorim, N. S. (2019). A review of hybrid integral transform solutions in fluid flow problems with heat or mass transfer and under Navier–Stokes equations formulation, *Numerical Heat Transfer, Part B: Fundamentals*. 76: 60–87.
- Cotta, R. M, Naveira-Cotta, C P, Knupp, D. C., Zotin, J. L. Z., Pontes, P. C., Almeida, A. P. (2018). Recent advances in computational-analytical integral transforms for convection-diffusion problems, *Heat and Mass Transfer*. 54; 2475–2496.
- Cotta, R. M. (1993). *Integral Transforms in Computational Heat and Fluid Flow*, CRC Press, Boca Raton, FL, 1993.
- Cotta, R. M. (1990). Hybrid numerical/analytical approach to nonlinear diffusion problems, *Numerical Heat Transfer, Part B: Fundamentals: An International Journal of Computation and Methodology*. 17; 217–226.
- Cotta, R. M. (1994). Benchmark results in computational heat and fluid flow: The integral transform method, *International Journal of Heat and Mass Transfer*. 37; 381–393.
- Cotta, R. M., Knupp, D. C., Quaresma, J.N. N., Lisboa, K. M., Naveira-Cotta, C P., Zotin, J. L. Z., Miyagawa, H. K. (2020). 50 Years of CFD in Engineering Sciences, in: Springer Singapore (Ed.), *Integral Transform Benchmarks of Diffusion, Convection Diffusion, and Conjugated Problems in Complex Domains.*, 1st ed., Springer Singapore: 719–750.
- Das R. and Kundu B. (2021). An Estimate of Heat Generation, Electric, and Magnetic Parameters From Temperature Fields in Porous Fins for Electronic Cooling Systems," *IEEE Transactions on Components, Packaging and Manufacturing Technology*, 11(8), 1250-1257.
- Das, R., Kundu, B., (2017). Prediction of Heat Generation in a Porous Fin from Surface Temperature," *Journal of Thermophysics and Heat Transfer*, 31(4), 781-790.
- Deshamukhya, T., Bhanja, D. Nath, S., Hazarika, S. A. (2018). Prediction of optimum design variables for maximum heat transfer through a rectangular porous fin using particle swarm optimization," *Journal of Mechanical Science and Technology*, journal article 32(9), 4495-4502.
- Ghasemi, S. E., Valipour, P., Hatami, M., Ganji, D. D. (2014). Heat transfer study on solid and porous convective fins with temperature-dependent heat generation using efficient analytical method," *Journal of Central South University*, 21(12), 4592-4598.
- Hassanzadeh, R., Bilgili, M. (2018). Assessment of Thermal Performance of Functionally Graded Materials in Longitudinal Fins," *Journal of Engineering Physics and Thermophysics*, 91(1), 79-88.
- Hatami, M., Ganji, D. D. (2013). Thermal performance of circular convective–radiative porous fins with different section shapes and materials," *Energy Conversion and Management*, 76, 185-193.
- Jany, P. and Bejan, A. (1988). Ernst Schmidt's approach to fin optimization: an extension to fins with variable conductivity and the design of ducts for fluid flow. *International Journal of Heat and Mass Transfer*, 31(8), 1635-1644.
- Jooma, R., C. Harley, C. (2017). Heat Transfer in a Porous Radial Fin: Analysis of Numerically Obtained Solutions," *Advances in Mathematical Physics*, 1658305.
- Kiwan, S. and Al-Nimr, M. A. (2000). Using Porous Fins for Heat Transfer Enhancement. *Journal of Heat Transfer*, 123(4), 790-795.

- Kiwan, S. and Alzahrany, M. S. (2007). Effect of Using Porous Inserts on Natural Convection Heat Transfer Between Two Concentric Vertical Cylinders. *Numerical Heat Transfer, Part A: Applications*, 53(8), 870-889.
- Knupp, D. C., Cotta, R. M, Naveira-Cotta, C P, ((2020). Conjugate Heat Transfer: Analysis Via Integral Transforms and Eigenvalue Problems, *Journal of Engineering Physics and Thermophysics*. 93; 60–73.
- Knupp, D. C., Cotta, R. M, Naveira-Cotta, C P, Kakaç, S. (2015). Transient conjugated heat transfer in microchannels: Integral transforms with single domain formulation, *International Journal of Thermal Sciences*. 88, 248–257.
- Kundu, B. (2010). Analytic method for thermal performance and optimization of an absorber plate fin having variable thermal conductivity and overall loss coefficient," *Applied Energy*, 87(7), 2243-2255.
- Kundu, B. and Yook, S. J. (2021). An accurate approach for thermal analysis of porous longitudinal, spine and radial fins with all nonlinearity effects – analytical and unified assessment," *Applied Mathematics and Computation*, 402, 126124.
- Kundu, B. Lee, K. S. (2016). A proper analytical analysis of annular step porous fins for determining maximum heat transfer," *Energy Conversion and Management*, 110,469-480.
- Mikhailov, M. D., Özisik, M. N. (1984). Unified analysis and solutions of heat and mass diffusion, John Wiley and Sons Inc, New York.
- Moitsheki, R. J. (2011). Steady heat transfer through a radial fin with rectangular and hyperbolic profiles," *Nonlinear Analysis: Real World Applications*, 12(2), 867-874.
- Moitsheki, R. J. (2011). Steady one-dimensional heat flow in a longitudinal triangular and parabolic fin," *Communications in Nonlinear Science and Numerical Simulation*, 16(10), 3971-3980.
- Moore, G. E.(2006). Cramming more components onto integrated circuits, Reprinted from *Electronics*, 38(8), April 19, 1965, pp.114 ff," *IEEE Solid-State Circuits Society Newsletter*, 11(3), 33-35.
- Moradi, A., Hayat, T., Alsaedi, A. (2014). Convection-radiation thermal analysis of triangular porous fins with temperature-dependent thermal conductivity by DTM," *Energy Conversion and Management*, 77, 70-77.
- Mosayebidorcheh, S., Ganji, D. D., M. Farzinpoor, M. (2014). Approximate solution of the nonlinear heat transfer equation of a fin with the power-law temperature-dependent thermal conductivity and heat transfer coefficient," *Propulsion and Power Research*, 3(1), 41-47.
- Oguntala, G. A., Abd-Alhameed, A. R., Sobamowo, M. G. and Danjuma, I. (2018). Performance, Thermal Stability and Optimum Design Analyses of Rectangular Fin with Temperature-Dependent Thermal Properties and Internal Heat Generation. *Journal of Computational Applied Mechanics*, 49(1), 37-43, 2018.
- Oguntala, G. A., Sobamowo, M. G. and Abd-Alhameed, R. (2019). Numerical analysis of transient response of convective-radiative cooling fin with convective tip under magnetic field for reliable thermal management of electronic systems," *Thermal Science and Engineering Progress*, 9, 289-298.
- Oguntala, G. A., Sobamowo, M. G. and Abd-Alhameed, R. (2020). A new hybrid approach for transient heat transfer analysis of convective-radiative fin of functionally graded material under Lorentz force," *Thermal Science and Engineering Progress*, 16, 100467,
- Oguntala, G. A., Sobamowo, M. G., Abd-Alhameed, R. and Noras, J. M. (2019). Numerical Study of Performance of Porous Fin Heat Sink of Functionally Graded Material for Improved Thermal Management of Consumer Electronics," *IEEE Transactions on Components, Packaging and Manufacturing Technology*, 1-1.
- Roy, P. K., Mondal, H., and A. Mallick, A. (2015). A decomposition method for convective–radiative fin with heat generation," *Ain Shams Engineering Journal*, 6(1), 307-313.
- Roy, R. and B. Kundu, B. (2018). Effects of fin shapes on heat transfer in microchannel heat sinks," *Heat Transfer—Asian Research*, 47(4), 646-659.

- Shokouhmand, H., Sattari, A., Hosseini-Doost, S. E., and Maghooli, A. (2018). Analysis of two-dimensional porous fins with variable thermal conductivity," *Heat Transfer—Asian Research*, vol. 47(2); 404-419.
- Snider A. D. and A. D. Kraus A. D. (1986), "Quest for the Optimum Longitudinal Fin Profile," in *American Society of Mechanical Engineers, Pressure Vessels and Piping Division (Publication) PVP*, 118, 43-48.
- Sobamowo, M. G. (2016). Thermal analysis of longitudinal fin with temperature-dependent properties and internal heat generation using Galerkin's method of weighted residual," *Applied Thermal Engineering*, 99; 1316-1330.
- Sobamowo, M. G. (2022). Combined Impacts of Fin Surface Inclination and Magnetohydrodynamics on the Thermal Performance of a Convective-Radiative Porous Fin. *Journal of Applied and Computational Mechanics*, 8(3), 940–948.
- Sobamowo, M. G., Dere, Z. O. and A. A. Yinusa, A. A. (2022). Nonlinear transient thermal analysis of a convective–radiative fin: A comparative study of two approximate analytical methods," *Decision Analytics Journal*, 5, 100133.
- Sobamowo, M. G., Oguntala, G. A., Yinusa, A. A. (2019). Nonlinear Transient Thermal Modeling and Analysis of a Convective-Radiative Fin with Functionally Graded Material in a Magnetic Environment. *Modelling and Simulation in Engineering*, 16, 7878564.
- Vahabzadeh, A., Ganji, D. D., Abbasi, M. (2015). Analytical investigation of porous pin fins with variable section in fully-wet conditions," *Case Studies in Thermal Engineering*, 5, 1-12.
- Yasong; J. S. M., Benwen, L. (2017). Simulation of combined conductive, convective and radiative heat transfer in moving irregular porous fins by spectral element method," *International Journal of Thermal Sciences*, 118; 475-487, 2017